

Low mass lepton pair production in hadron collisions

E.L. Berger and M. Klasen ^{a*}

^aHEP Theory Group, Argonne National Laboratory, 9700 South Cass Avenue, Argonne, IL 60439, USA

The hadroproduction of lepton pairs with mass Q and transverse momentum Q_T can be described in perturbative QCD by the same partonic subprocesses as prompt photon production. We demonstrate that, like prompt photon production, lepton pair production is dominated by quark-gluon scattering in the region $Q_T > Q/2$. This leads to sensitivity to the gluon density in kinematical regimes that are accessible both at collider and fixed target experiments while eliminating the theoretical and experimental uncertainties present in prompt photon production.

1. INTRODUCTION

The production of lepton pairs in hadron collisions $h_1 h_2 \rightarrow \gamma^* X; \gamma^* \rightarrow l\bar{l}$ proceeds through an intermediate virtual photon and its subsequent leptonic decay. Traditionally, interest in this Drell-Yan process has concentrated on lepton pairs with large mass Q which allows for the application of perturbative QCD and the extraction of the antiquark density in the proton [1].

Prompt photon production $h_1 h_2 \rightarrow \gamma X$ can be calculated in perturbative QCD if the transverse momentum Q_T of the photon is sufficiently large. This process then provides essential information on the gluon density in the proton at large x [2]. Unfortunately, it suffers from considerable fragmentation, isolation, and intrinsic transverse momentum uncertainties. Alternatively, the gluon density can be constrained from the production of jets with large transverse momentum at hadron colliders [3], which however suffers from ambiguous information coming from different experiments and colliders.

In this paper we demonstrate that, like prompt photon production, lepton pair production is dominated by quark-gluon scattering in the region $Q_T > Q/2$. This leads to sensitivity to the gluon density in kinematical regimes that are accessible both at collider and fixed target experiments while eliminating the theoretical and experimental uncertainties.

In Sec. 2, we briefly discuss the relationship between virtual and real photon production in hadron collisions in next-to-leading order QCD. In Sec. 3 we present our numerical results, and Sec. 4 contains a summary.

2. NEXT-TO-LEADING ORDER QCD FORMALISM

In leading order (LO) QCD, two partonic subprocesses contribute to the production of virtual and real photons with non-zero transverse momentum: $q\bar{q} \rightarrow \gamma^{(*)}g$ and $qg \rightarrow \gamma^{(*)}q$. The cross section for lepton pair production is related to the cross section for virtual photon production through the leptonic branching ratio of the virtual photon $\alpha/(3\pi Q^2)$. The virtual photon cross section reduces to the real photon cross section in the limit $Q^2 \rightarrow 0$.

The next-to-leading order (NLO) QCD corrections arise from virtual one-loop diagrams interfering with the LO diagrams and from real emission diagrams. At this order processes with incident gluon pairs (gg), quark pairs (qq), and non-factorizable quark-antiquark ($q\bar{q}_2$) processes contribute also. Singular contributions are regulated in $n = 4 - 2\epsilon$ dimensions and removed through $\overline{\text{MS}}$ renormalization, factorization, or cancellation between virtual and real contributions. An important difference between virtual and real photon production arises when a quark emits a collinear photon. Whereas the collinear emission of a real photon leads to a $1/\epsilon$ singularity that has to

*Supported by the U.S. Department of Energy, Division of High Energy Physics, under Contract W-31-109-ENG-38.

be factorized into a fragmentation function, the collinear emission of a virtual photon gives a finite logarithmic contribution since it is regulated naturally by the photon virtuality Q . In the limit $Q^2 \rightarrow 0$ the NLO virtual photon cross section reduces to the real photon cross section if this logarithm is replaced by a $1/\epsilon$ pole. A more detailed discussion can be found in [4].

The situation is completely analogous to hard photoproduction where the photon participates in the scattering in the initial state instead of the final state. For real photons, one encounters an initial-state singularity that is factorized into a photon structure function. For virtual photons, this singularity is replaced by a logarithmic dependence on the photon virtuality Q [5].

3. NUMERICAL RESULTS

In this section we present numerical results for the production of lepton pairs in $p\bar{p}$ collisions at the Tevatron with center-of mass energy $\sqrt{S} = 1.8$ and 2.0 TeV and in pH^2 collisions at fixed target experiments with $\sqrt{S} = 38.8$ GeV. We analyze the invariant cross section $Ed^3\sigma/dp^3$ averaged over the rapidity interval $-1.0 < y < 1.0$ at the Tevatron and averaged over the scaled longitudinal momentum interval $0.1 < x_F < 0.3$ at fixed target experiments. We integrate the cross section over various intervals of Q and plot it as a function of the transverse momentum Q_T . Our predictions are based on a NLO QCD calculation [9] and are evaluated in the $\overline{\text{MS}}$ renormalization scheme. The renormalization and factorization scales are set to $\mu = \mu_f = \sqrt{Q^2 + Q_T^2}$. If not stated otherwise, we use the CTEQ4M parton distributions [10] and the corresponding value of Λ in the two-loop expression of α_s with four flavors (five if $\mu > m_b$). The Drell-Yan factor $\alpha/(3\pi Q^2)$ for the decay of the virtual photon into a lepton pair is included in all numerical results.

In Fig. 1 we display the NLO QCD cross section for lepton pair production at the Tevatron at $\sqrt{S} = 1.8$ TeV as a function of Q_T for four regions of Q . The regions of Q have been chosen carefully to avoid resonances, *i.e.* between the ρ and the J/ψ resonances, between the J/ψ and the Υ resonances, above the Υ 's, and a high

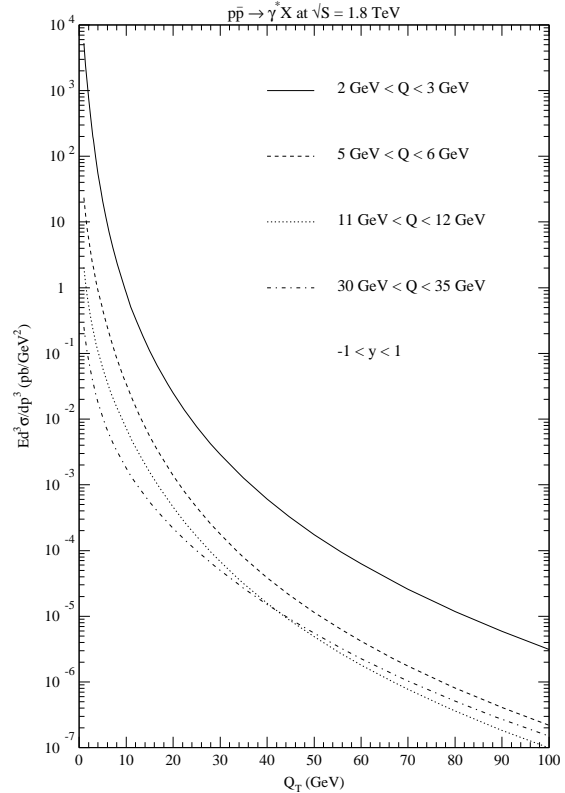


Figure 1. Invariant cross section $Ed^3\sigma/dp^3$ as a function of Q_T for $p\bar{p} \rightarrow \gamma^* X$ at $\sqrt{S} = 1.8$ TeV in non-resonance regions of Q . The cross section falls with the mass of the lepton pair Q and, more steeply, with its transverse momentum Q_T .

mass region. The cross section falls both with the mass of the lepton pair Q and, more steeply, with its transverse momentum Q_T . Unfortunately, no data are available yet from the CDF and D0 experiments. However, data exist for prompt photon production out to $Q_T \simeq 100$ GeV, where the cross section is about 10^{-3} pb/GeV². It should therefore be possible to analyze Run I data for lepton pair production up to at least $Q_T \simeq 30$ GeV where one can probe the parton densities in the proton up to $x_T = 2Q_T/\sqrt{S} \simeq 0.03$. The UA1 collaboration measured the transverse momentum distribution of lepton pairs at $\sqrt{S} = 630$

GeV up to $x_T = 0.13$ [11], and their data agree well with our theoretical results [4].

The fractional contributions from the qg and $q\bar{q}$ subprocesses up through NLO are shown in Fig. 2. It is evident from Fig. 2 that the qg sub-

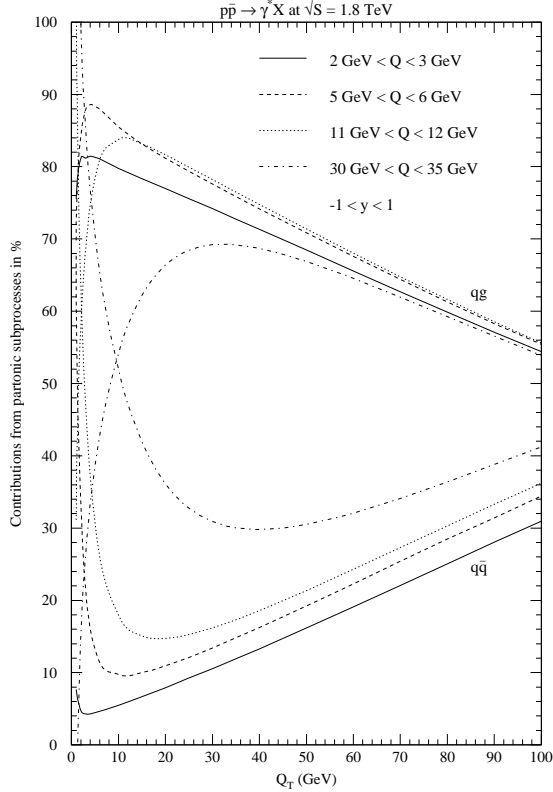


Figure 2. Contributions from the partonic subprocesses qg and $q\bar{q}$ to the invariant cross section $Ed^3\sigma/dp^3$ as a function of Q_T for $p\bar{p} \rightarrow \gamma^* X$ at $\sqrt{S} = 1.8$ TeV. The qg channel clearly dominates in the region $Q_T > Q/2$.

process is the most important subprocess as long as $Q_T > Q/2$. The dominance of the qg subprocess diminishes somewhat with Q , dropping from over 80 % for the lowest values of Q to about 70 % at its maximum for $Q \simeq 30$ GeV. In addition, for very large Q_T , the significant luminosity associated with the valence dominated \bar{q} density in $p\bar{p}$

reactions begins to raise the fraction of the cross section attributed to the $q\bar{q}$ subprocesses.

Data obtained by the Fermilab E772 collaboration [12] from an 800 GeV proton beam incident on a deuterium target are shown in Fig. 3 along with theoretical calculations. For our anal-

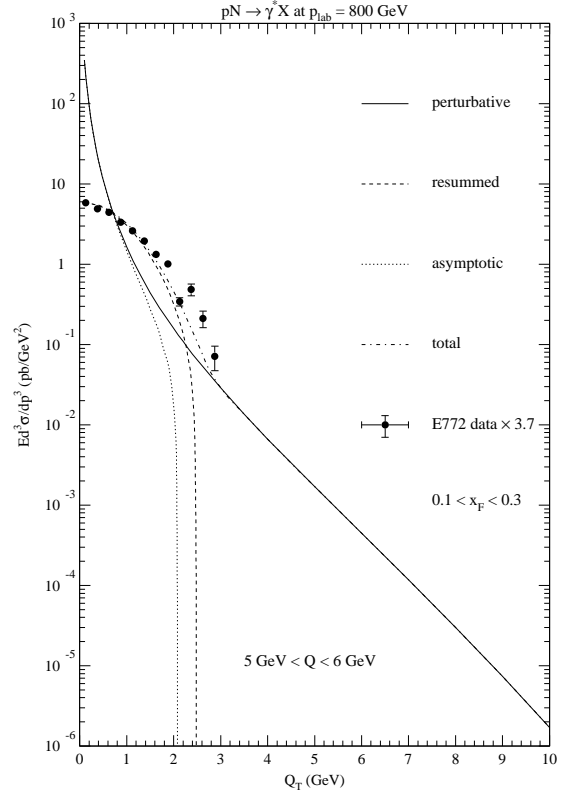


Figure 3. Invariant cross section $Ed^3\sigma/dp^3$ as a function of Q_T for $pN \rightarrow \gamma^* X$ at $p_{\text{lab}} = 800$ GeV in the region between the J/ψ and Υ resonances. The NLO perturbative cross section (solid) is shown along with the all-orders resummed expectation (dashed), the asymptotic result (dotted), and a matched expression (dot-dashed). The data are from the Fermilab E772 collaboration.

ysis we have chosen a lepton pair mass region between the J/ψ and Υ resonances. The solid

line shows the purely perturbative NLO expectation. The transition to low Q_T can be described by the soft-gluon resummation formalism and is shown in the dashed curve in Fig. 3 [7,8]. The resummed result can be expanded in a power series in α_s asymptotically around $Q_T = 0$. Its NLO component (dotted curve) can then be matched to the perturbative result (dot-dashed curve) [9]. From Fig. 3 it becomes clear that resummation is not needed and fixed order perturbation theory can be trusted when $Q_T > Q/2$. Unfortunately, the data from E772 do not extend into this region. However, the cross section should be measurable in forthcoming experiments down to 10^{-3} pb/GeV², *i.e.* out to at least $Q_T \simeq 6$ GeV or $x_T \simeq 0.31$ where the gluon density is poorly constrained now.

In Fig. 4 we demonstrate that in fixed target experiments also the lepton pair cross section is dominated by quark-gluon scattering at the level of 80 % once $Q_T \simeq Q$. The results in Fig. 4 also prove that subprocesses other than those initiated by the $q\bar{q}$ and qg initial channels are of negligible import.

We will now turn to a previously unpublished study of the sensitivity of collider and fixed target experiments to the gluon density in the proton. The full uncertainty in the gluon density is not known. Here we estimate this uncertainty from the variation of different recent parametrizations. We choose the latest global fit by the CTEQ collaboration (5M) as our point of reference [3] and compare it to their preceding analysis (4M [10]) and to a fit with a higher gluon density (5HJ) intended to describe the CDF (and D0) jet data at large transverse momentum. We also compare to global fits by MRST [2], who provide three different sets with a central, higher, and lower gluon density, and to GRV98 [13]². For this study we update the Tevatron center-of-mass energy to Run II conditions ($\sqrt{S} = 2.0$ TeV) which increases the invariant cross section for the production of lepton pairs with mass $5 \text{ GeV} < Q <$

6 GeV by 5 % at low $Q_T \simeq 1$ GeV and 20 % at high $Q_T \simeq 100$ GeV.

In Fig. 5 we plot the cross section for lepton pairs between the J/ψ and Υ resonances at Run II of the Tevatron which should be measurable up to at least $Q_T \simeq 30$ GeV ($x_T \simeq 0.03$). For the CTEQ parametrizations we find that the cross section increases from 4M to 5M by 2.5 % ($Q_T = 30$ GeV) to 5 % ($Q_T = 10$ GeV) and from 5M to 5HJ by 1 % in the whole Q_T -range. The largest differences to CTEQ5M are obtained with GRV98 at low Q_T (minus 10 %) and with MRST(g \uparrow) at large Q_T (minus 7%).

A similar analysis for conditions as in Fermilab's E772 experiment is shown in Fig. 6. In fixed target experiments one probes substantially larger regions of x_T than in collider experiments. Therefore one expects a much larger sensitivity to the gluon distribution in the proton. Indeed we find that CTEQ5HJ increases the cross section by 7 % (26 %) w.r.t. CTEQ5M at $Q_T = 3$ GeV ($Q_T = 6$ GeV) and even by 134 % at $Q_T = 10$ GeV. For MRST(g \downarrow) the CTEQ5M cross section drops by 17 %, 40 %, and 59 % at these three values of Q_T .

4. SUMMARY

In summary, we have demonstrated that the production of Drell-Yan pairs with low mass and large transverse momentum is dominated by gluon initiated subprocesses. In contrast to prompt photon production, uncertainties coming from fragmentation, isolation, and intrinsic transverse momentum are absent. The hadroproduction of low mass lepton pairs is therefore an advantageous source of information on the gluon density in the proton at large x in collider experiments and even more in fixed target experiments. Massive lepton pair production data could provide new insights into the parametrization and size of the gluon density.

Acknowledgement

It is a pleasure to thank L.E. Gordon for his collaboration.

²In this set a purely perturbative generation of heavy flavors (charm and bottom) is assumed. Since we are working in a massless approach, we resort to the GRV92 parametrization for the charm contribution [14] and assume the bottom contribution to be negligible.

REFERENCES

1. S.D. Drell and T. Yan, Phys. Rev. Lett. **25** (1970) 316.
2. A.D. Martin, R.G. Roberts, W.J. Stirling and R.S. Thorne, Eur. Phys. J. **C4** (1998) 463 hep-ph/9803445.
3. H.L. Lai *et al.* [CTEQ Collaboration], hep-ph/9903282.
4. E.L. Berger, L.E. Gordon and M. Klasen, Phys. Rev. **D58** (1998) 074012 hep-ph/9803387.
5. M. Klasen, G. Kramer and B. Pötter, Eur. Phys. J. **C1** (1998) 261 hep-ph/9703302.
6. P.B. Arnold and M.H. Reno, Nucl. Phys. **B319** (1989) 37 and Erratum Nucl. Phys. **B330** (1990) 284.
7. J.C. Collins, D.E. Soper and G. Sterman, Nucl. Phys. **B250** (1985) 199.
8. G.A. Ladinsky and C.P. Yuan, Phys. Rev. **D50** (1994) 4239 hep-ph/9311341.
9. P.B. Arnold and R.P. Kauffman, Nucl. Phys. **B349** (1991) 381.
10. H.L. Lai *et al.*, Phys. Rev. **D55** (1997) 1280 hep-ph/9606399.
11. C. Albajar *et al.* [UA1 Collaboration], Phys. Lett. **209B** (1988) 397.
12. P.L. McGaughey *et al.* [E772 Collaboration], Phys. Rev. **D50** (1994) 3038. The normalization of the published data seems incorrect. We have multiplied the published cross sections by a factor 3.7, consistent with information provided to us by J. Moss (private communication).
13. M. Glück, E. Reya and A. Vogt, Eur. Phys. J. **C5** (1998) 461 hep-ph/9806404.
14. M. Glück, E. Reya and A. Vogt, Z. Phys. **C53** (1992) 127.

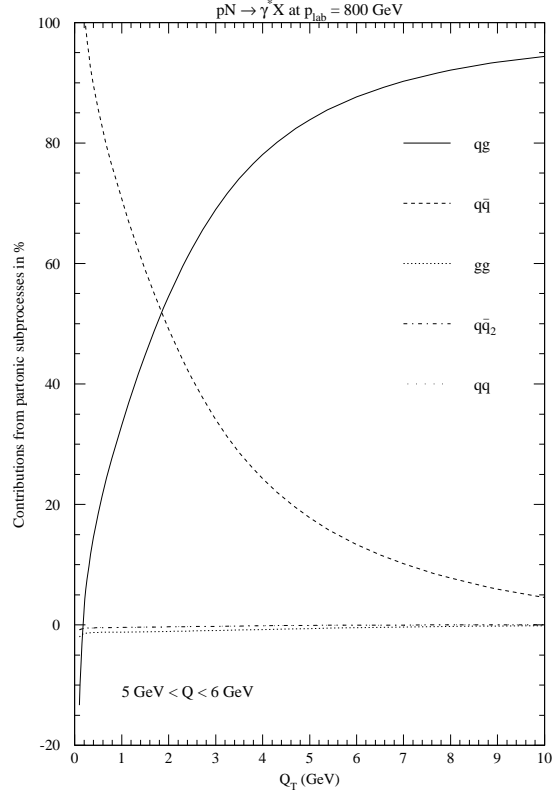


Figure 4. Contributions from the NLO QCD partonic subprocesses to the invariant cross section $Ed^3\sigma/dp^3$ as a function of Q_T for $pN \rightarrow \gamma^* X$ at $p_{\text{lab}} = 800$ GeV. qg (solid) dominates over $q\bar{q}$ (dashed) at the level of 80 % once $Q_T \simeq Q$, and the pure NLO QCD processes gg (dotted), $q\bar{q}_2$ non-factorizable parts (dot-dashed), and qq (wide dots) are negligible.

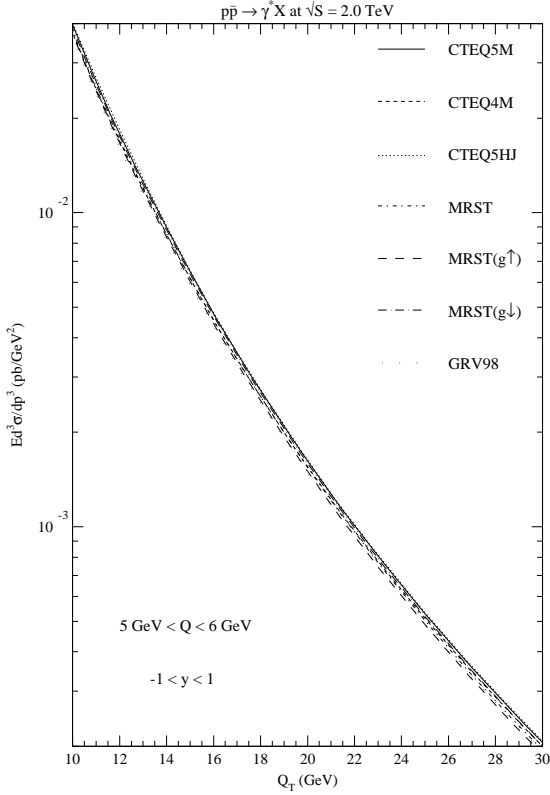


Figure 5. Invariant cross section $Ed^3\sigma/dp^3$ as a function of Q_T for $p\bar{p} \rightarrow \gamma^* X$ at $\sqrt{S} = 2.0$ TeV in the region between the J/ψ and Υ resonances. The largest differences from CTEQ5M are obtained with GRV98 at low Q_T (minus 10 %) and with MRST($g\uparrow$) at large Q_T (minus 7 %).

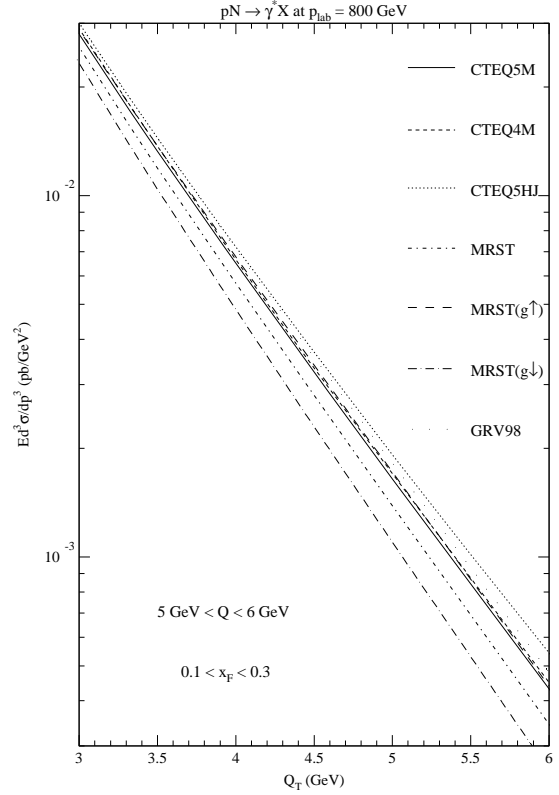


Figure 6. Invariant cross section $Ed^3\sigma/dp^3$ as a function of Q_T for $pN \rightarrow \gamma^* X$ at $p_{\text{lab}} = 800$ GeV. The cross section is highly sensitive to the gluon distribution in the proton in regions of x_T where it is poorly constrained.